The collapse transition of semiflexible polymers. A Monte Carlo simulation of a model system

Andrzej Kolinski,[a] Jeffrey Skolnick,[b] and Robert Yaris
Institute of Macromolecular Chemistry, Department of Chemistry, Washington University, St. Louis, Missouri 63130

(Received 25 April 1986; accepted 13 June 1986)

Monte Carlo simulations have been performed on a diamond lattice model of semiflexible polymers for a range of flexibilities and a range of chain lengths from 50 to 800 segments. The model includes both repulsive (excluded volume) and attractive segment–segment interactions. It is shown that the polymers group into two classes, "flexible" and "stiff." The flexible polymers exhibit decreasing chain dimensions as the temperature decreases with a gradual collapse from a loose random coil, high temperature state to a dense random coil, low temperature state. The stiffer polymers, on the other hand, exhibit increasing chain dimensions with decreasing temperature until at a critical temperature there is a sudden collapse to an ordered high density, low temperature state. This difference is due to the relative strength of the segment–segment attractive interactions compared to the energetic preference for a *trans* conformational state over a *gauche* state. When the attractive interaction is relatively strong (flexible case) the polymer starts to collapse before rotational degrees of freedom freeze out, leading to a disordered dense state. When the attractive interaction is relatively weak (stiff case) the polymer starts to freeze out rotational degrees of freedom before it finally collapses to a highly ordered dense state.

I. INTRODUCTION

The conformation of a single long-chain polymer in dilute solution is often compared to a random walk in three-dimensional space. As is well known, the real problem, however, is complicated by the non-Markovian character of the polymer conformation due to the physical impossibility of two polymer units, separated by some distance down the chain, occupying the same small volume element. This so-called excluded volume effect depends on the strength of the "long-range" interactions in the polymer coil. The term long-range refers to a large distance along the chain contour, but not to a large separation in space. Actually, the most common case of uncharged polymers requires consideration of very small spatial distances, comparable to the size of a single chain element. It was first shown by Flory[1] that in a good solvent and/or at high temperatures, the excluded volume effect leads to a large increase of the chain dimensions in comparison with an ideal random walk. In this case the mean square end-to-end separation $\langle R^2 \rangle$ scales as

$$\langle R^2 \rangle \sim n^{6/5}, \tag{1}$$

with n the chain length. A similar relation holds for the mean-square radius of gyration of the polymer coil $\langle S^2 \rangle$ which is more easily available from experimental measurements. Flory's result has been essentially confirmed by other more rigorous treatments of flexible polymers based on mean-field theory,[2–5] renormalization group methods,[6] exact enumerations on a lattice for short chains,[7–9] and Monte Carlo simulations for much longer polymers.[10–14] Local, short-range interactions down the chain can be included in the proportionality constant if the chain length n is not too small.

When the temperature decreases, or when a good solvent is replaced by a poor one (in a poor solvent the attractive interactions between polymer segments dominate over the segment–solvent interaction) the chain dimensions decrease, and at the θ temperature[1] one obtains the random walk result

$$\langle R^2 \rangle \sim n. \tag{2}$$

A further temperature decrease leads to a collapse of the polymer coil to a more compact state. There is some evidence[6,12,15] that in the limit of long flexible polymers the resulting globule can be characterized by

$$\langle R^2 \rangle \sim n^{2/3}. \tag{3}$$

Domb[16] found that in the long chain limit the collapse transition temperature was identical to the θ temperature. He argued that the collapse transition was first order. More recent theoretical analysis by Moore[17] and the mean-field theory of Sanchez[3] predict a second-order, Landau type transition. Sanchez's work, as well as other theoretical considerations[17–19] and numerical tests[12,13] show that even close to the θ temperature the polymer conformation differs considerably from a Markov random walk and the distribution of the polymer segments within the coil is relatively far from the Gaussian distribution of an ideal unrestricted chain.

It should be pointed out that the above conclusions concerning the thermodynamic character of the collapse transitions have built in (for the case of long polymers) the implicit assumption of substantial flexibility of the chain backbone. Because there is some theoretical[6(b),20–23] and experimental[24] evidence of the large importance of local chain stiffness in the excluded volume effect, it is possible that chain stiffness can affect the character of the collapse transition. Indeed, a mean-field lattice treatment incorporating ternary interactions in a virial expansion leads to qualitatively different predictions for polymers having different flexibility. In

[a] Permanent address: Department of Chemistry, University of Warsaw, 02-093 Warsaw, Poland.
[b] Alfred P. Sloan Foundation Fellow.

 0021-9606/86/183585-13$02.10

the analytical work of Post and Zimm,[21] it has been shown that relatively stiff polymers, like DNA, should collapse with a sharp discontinuous change of coil size, while more flexible, synthetic polymers will undergo a collapse transition with a gradual change of chain dimensions as a function of temperature. Moreover the results of Post and Zimm are not restricted to the case of the long chain limit, but also hold for real polymer chains with a finite degree of polymerization.

In the present Monte Carlo (MC) computations, we study the effect of chain stiffness in polymers of finite length on the excluded volume effect and also on the character of the collapse transition. Within the framework of a lattice model, we make a reasonable approximation to the interactions between polymer segments and include both the repulsive and attractive parts of the potential. To our knowledge this is the first consistent numerical analysis of the excluded volume effect together with the effect of local chain stiffness that has been applied to the collapse transition in model polymers of reasonable length. Within the statistical accuracy of the Monte Carlo method, and in the range of the validity of lattice models, the results should be exact. Therefore, the present analysis should have relevance to the properties of real dilute polymer systems.

One further feature of the collapse transition which we investigated was the nature of the collapsed state. As we shall show, for flexible polymers the collapse is to an essentially Gaussian, tight random coil as one would expect. However, for finite length polymers which have a considerable degree of stiffness, the polymer collapses into an ordered state. This collapse into an ordered state from a random coil is similar to the denatured to native transition in globular proteins. The physical origin of this ordered collapse transition is discussed below.

The remainder of the paper is arranged in the following way. In Sec. II the assumptions of the model (subsection A) and the sampling MC procedure used (subsection B) are described. Then, the simulation results are discussed in Sec. III. Subsection A describes excluded volume effects in semiflexible polymers. We compare our results with third order mean-field theory in subsection B. In the subsection C, the effect of chain stiffness on the structure of the collapsed, low temperature, phase is discussed. The major conclusions of the present work are summarized in Sec. IV.

II. MODEL AND SAMPLING PROCEDURE

A. Description of the model

The model under consideration is the diamond lattice representation[25,26] of the rotational isomeric states (RIS) model of the polymer conformation with excluded volume. For computational convenience we have assigned the bond vectors the following form: $l_i = \beta_k$ for bonds starting from an odd lattice point, and $l_i = -\beta_k$ for bonds starting from an even lattice point. The index i enumerates the bonds down the chain where $i = 1,2,\ldots,n-1$ and the β_k with $k = 1, 2, 3, 4$ are the diamond lattice vectors. Using an integer representation of all the polymer beads, the set $\{\beta_k\}$ has the following form:

$$\beta_1 = [1,1,1],\ \beta_2 = [1,-1,-1],$$
$$\beta_3 = [-1,1,-1],\ \text{and}\ \beta_4 = [-1,-1,1].$$

Every sequence of the three bonds defines an isomeric state for which, with a constant tetrahedral bond angle, there are three available conformational states: *t*, *trans*, g_-, *gauche* minus, and g_+, *gauche* plus. The conformation of the entire chain requires that $n-3$ rotational degrees of freedom be specified. A symmetric rotational potential has been assumed in the present computation, where ϵ_g is the energy separation of a *gauche* and a *trans* state. Thus the statistical weights of the rotational isomeric states are

$$\omega(t) = 1, \omega(g+) = \omega(g-) = \exp(-\epsilon_g/k_B T)\,. \tag{4}$$

We consider only $\epsilon_g \geqslant 0$. The interactions between polymer beads are described by the potential

$$V(r_{ij}) = \begin{cases} \infty; & r_{ij} = 0, \quad i \neq j \\ \epsilon_a; & r_{ij} = l, \quad |i-j| \neq 1\,, \\ 0; & r_{ij} > l \end{cases} \tag{5}$$

where r_{ij} is the distance between ith and jth beads in the chain, l is a lattice bond distance and is equal to $3^{1/2}$ in our units, and ϵ_a is the attractive parameter; only $\epsilon_a \leqslant 0$ has been considered. Hence, any conformation with m_g *gauche* states and m_a contacts between nonbonded polymer segments, with no multiple occupancy of any lattice site, has the configurational energy

$$E = m_g \epsilon_g + m_a \epsilon_a\,. \tag{6}$$

For the purpose of convenient comparison of the properties of chains of various lengths we define the average density ν of nearest nonbonded neighbors. The numerical value of ν is the same as the average number of binary contacts per polymer bead for the lattice under consideration (coordination number $q = 4$) and

$$\nu = \frac{2m_a}{n(q-2)+2}\,. \tag{7}$$

Similarly, we define the fraction of *gauche* states per degree of rotational freedom

$$f_g = m_g/(n-3)\,. \tag{8}$$

Both the parameters ν and f_g measure the local packing and conformational order within the polymer, with convenient values for limiting cases. Namely $\nu = 0$ and $f_g = 0$ for a rigid rod molecule, and $\nu = 1$ for a Hamiltonian walk, while the value of f_g depends on the geometric properties of the Hamiltonian walk.[27]

B. Monte Carlo sampling procedure

There are a variety of Monte Carlo procedures which have been applied for sampling self-avoiding random walks (SAW's) of various types. Probably the most commonly used are the simple sampling (SS) method,[14] Rosenbluths' method[28] (RR), and the scanning method[29] which extends the RR procedure. Though all of these static sampling methods have been very successful in numerous applications they are unsuited to the present problem for the following reason. We expect that the collapsed structure of semiflexible polymers, with a high preference for *trans* conformations, could

be partially ordered, presumably with a high local density of polymer segments. Therefore we need a sampling procedure that possesses the ability to sample with similar accuracy the broad expanse of configurational space available to a random coil as well as the much smaller region of configurational space accessible to a collapsed structure. This seems to be difficult to achieve by means of a static method. Hence a dynamic sampling technique[12] has been used, within the framework of an asymmetric Metropolis scheme.

Let us assume that the polymer chain is in some configuration. Then one can perform a small modification of the chain conformation which is associated with the energy change $\Delta E_{ij} = E_j - E_i$, where E_i is the configurational energy [Eq. (6)] of the "old" state and E_j is the energy of the "new" one. The new conformation is then accepted provided the Boltzmann factor connected with the micromodification is larger than a random number chosen from a uniform distribution over the range (0,1). This leads to a probability of acceptance of the trial conformation

$$p_{ij} = \min\{1, \exp(-\Delta E_{ij}/k_B T)\} \tag{9}$$

and the distribution of states tends to an equilibrium Boltzmann distribution in the limit of long MC sequences.

Two versions of the sampling MC algorithms have been used. In the first one the following modifications of the chain conformation were employed:

(i) "reptation" type motion, where a randomly chosen end segment is clipped off and then added at a random direction to the opposite chain end;

(ii) a random rotation of a small end portion of the chain (1–2 bonds);

(iii) three-bond kink motions, resulting from the permutation of the chain segments in a randomly chosen part of the chain (only a sequence comprising a *gauche* conformation could be affected by this kind of modification—see Ref. 12 for some details).

Successions of the micromodifications (i)–(iii) were randomly mixed, with an average frequency of attempts (i):(ii):(iii) :: 1:1: xn, where x is some arbitrary fractional number (we used x ranging from 0 to 0.1). Thus for our sampling algorithm the major mode of chain motion is reptation because of its high efficiency in sampling configurational space.

The second algorithm we used differs from the first one in that the direction of reptation down the chain contour is kept unchanged until the first unsuccessful move. Then the reptation direction is switched to the opposite direction. Both MC algorithms give the same results, but the second seems to be more efficient, especially in the low temperature range.

For each set of the initial parameters of the model (i.e., n, $\epsilon_g/k_B T$, and $\epsilon_a/k_B T$) long runs consisting of 0.5–3.0×10^7 reptation type steps, with a corresponding number of other micromodifications, have been performed. The chain conformations have been stored in two complementary lists; the first contained a sequential set of the Cartesian coordinates of the polymer beads, and the second was the explicit occupancy list in the periodic $L\times L\times L$ MC box. The last list allows the fast detection of the mutual contacts of the polymer segments. The finite size of the MC box does not affect the results obtained because the edge length L has been set to 100 for chain lengths $n \leqslant 400$, to $L = 124$ for the more expanded conformations of chains with $n = 400$, and to $L = 198$ for the limited simulations made for chain length $n = 800$. Therefore the unphysical interaction of a chain with its image resulting from periodic boundary conditions are at worst highly improbable and in fact impossible in most cases.

Various properties of the chain were recorded every 250–500 cycles of the simulation algorithm. Thus, the resulting number of states used for calculating the equilibrium properties of the system varied from 2×10^4 to 6×10^4. All measured quantities were calculated as arithmetic averages over such a trajectory, due to equilibrium character of the sampling procedure employed. Every sampling MC run was preceded by a suitable equilibration run to ensure that system was really in thermal equilibrium. Much shorter runs were observed to be necessary for the relaxation of the system (from one temperature to another one) than those used in sampling. At higher temperatures, the sampling interval we used (250–500 cycles) gives good statistical independence of the sampled states, while at lower temperatures, since the evolution of the system is slowed down by strong intrachain interactions (below the collapse transition), the statistics are probably somewhat poorer. Therefore below the collapse transition successive "photographs" of the chain conformation cannot be considered as statistically uncorrelated. For that reason "cooling" cycles followed by "heating" cycles were performed several times in the vicinity of the phase transition for a given set of initial parameters of the stiff polymer chains, using a different stream of random numbers for each cycle. This allowed us to estimate the level of statistical importance of the results and the stability and uniqueness of the structure of the dense collapsed states.

III. RESULTS AND DISCUSSION

A. Conformation of the model polymers and the collapse transition

Generally speaking the conformation of the polymer chain in solution depends on the chain length and the short- and long-range interactions. Various parameters describing the local ordering of the polymer segment within the coil, as well as the global conformational characteristics were estimated from MC simulations described in the previous section. The size of the polymer coil was measured using the mean-square end-to-end separation $\langle R^2\rangle$;

$$\langle R^2\rangle = \langle(\mathbf{r}_n - \mathbf{r}_1)^2\rangle, \tag{10}$$

and the mean-square radius of gyration $\langle S^2\rangle$;

$$\langle S^2\rangle = \frac{1}{n}\left\langle \sum_{i=1}^{n} (\mathbf{r}_i - \mathbf{r}_{CM})^2 \right\rangle, \tag{11}$$

where $\mathbf{r}_i$ is the vector locating the ith bead in the chain, $\mathbf{r}_{CM}$ is the vector locating the center of mass of the coil, and $\langle\ \rangle$ denotes an ensemble average over the trajectory of the MC run. Higher moments of the end-to-end separation and the radius of gyration, as well as the polymer segment density

TABLE I. Average properties of chains of length $n = 50$.

ϵ_g/k_BT	$\langle R^2\rangle$	$\langle S^2\rangle$	$\langle \nu\rangle$	$\langle f_g\rangle$
		$\lvert\epsilon_g/\epsilon_a\rvert = 4$		
0.0	410.5	64.26	0.0530	0.6329
1.0	616.6	94.49	0.0284	0.4191
2.0	1211.7	166.2	0.0144	0.2146

TABLE II. Average properties of chains of length $n = 100$.

ϵ_g/k_BT	$\langle R^2\rangle$	$\langle S^2\rangle$	$\langle \nu\rangle$	$\langle f_g\rangle$
		$\lvert\epsilon_g/\epsilon_a\rvert = 4$		
0.0	941.8	148.5	0.0576	0.6297
1.0	1394.5	217.8	0.0330	0.4169
2.0	2641.5	393.5	0.0202	0.2171

TABLE III. Average properties of chains of length $n = 200$.

ϵ_g/k_BT	$\langle R^2\rangle$	$\langle S^2\rangle$	$\langle \nu\rangle$	$\langle f_g\rangle$
		$\epsilon_a = 0$		
0.0	2148(11)[a]	344.1(3.9)	0.0595(7)	0.6290(8)
0.1	2246	354.5	0.0553	0.6080
0.25	2334	371.3	0.0494	0.5770
0.5	2584	411.3	0.0386	0.5209
0.625	2707	432.9	0.0344	0.4924
0.8	2944	470.5	0.0280	0.4517
1.0	3288	521.2	0.0223	0.4083
1.25	3814	606.3	0.0158	0.3534
1.6	4976	772.1	0.0093	0.2790
2.0	6435	1008.7	0.0048	0.2088
2.5	10622	1548.6	0.0020	0.1389
		$\lvert\epsilon_g/\epsilon_a\rvert = 4$		
0.5	2491	396.6	0.0477	0.5252
0.8	2861	429.9	0.0409	0.4618
1.0	2955	477.0	0.0361	0.4169
1.5	3611	577.6	0.0287	0.3119
1.6	4262	675.7	0.0264	0.2886
1.8	4669	738.4	0.0250	0.2511
2.0	5283	829.6	0.0282	0.2165
2.1	5444	855.6	0.0373	0.1980
2.2($T\downarrow$)[b]	6076	951.6	0.0373	0.1818
2.2($T\uparrow$)[c]	(654)[d]	288.9	0.4643	0.0888
2.3	(1114)	294.1	0.4387	0.0989
2.4	(125)	317.9	0.4513	0.0633
		$\lvert\epsilon_g/\epsilon_a\rvert = 3$		
0.45	2314	370.9	0.0529	0.5386
0.6	2386	386.9	0.0489	0.5036
0.9	2622	419.9	0.0458	0.4432
1.2	2977(50)	482.1(7.1)	0.0422(2)	0.3774(2)
1.4	3245(49)	529.8(7.7)	0.0402(1)	0.3339(2)
1.5	3356(14)	544.2(3.0)	0.0406(2)	0.3150(3)
1.65	3635	585.8	0.0454	0.2864
1.74	3901	635.2	0.0449	0.2680
1.8	3751	613.0	0.0631	0.2531
1.83	3488	576.9	0.0791	0.2450
1.86	3376	566.0	0.0722	0.2414
1.89($T\downarrow$)[b]	2833	488.4	0.1387	0.2188
1.89($T\uparrow$)[c]	(1831.8)	389.4	0.2941	0.1693
1.92	(622.1)	189.7	0.4752	0.1153
1.95	(914.0)	275.9	0.4128	0.1256
2.1	(834.5)	326.8	0.3887	0.1287
2.4	(316.9)	289.3	0.4747	0.0816
		$\lvert\epsilon_g/\epsilon_a\rvert = 2$		
0.5	2225	357.8	0.0603	0.5342
0.6	2230	362.3	0.0619	0.5123
0.75	2186	356.6	0.0648	0.4821
1.0	2282	374.2	0.0713	0.4292
1.1	2167	360.2	0.0777	0.4022
1.16	2115(43)	350.9(4.8)	0.0851(30)	0.3948(17)
1.21	1988(47)	338.7(3.6)	0.0914(7)	0.3911(36)
1.28	1908(35)	321.1(9.2)	0.1008(27)	0.3728(21)
1.32	1873	314.7	0.1029	0.3722
1.4	1437	257.1	0.1422	0.3496
1.5	1041	185.8	0.2459	0.3130
1.6	743	135.5	0.3683	0.2635
1.8	804	156.7	0.3750	0.2289
		$\lvert\epsilon_g/\epsilon_a\rvert = 4/3$		
0.2	2078	333.6	0.0658	0.5963
0.4	1960	319.3	0.0769	0.5593
0.52	1879	307.7	0.0823	0.5369
0.6	1821	299.4	0.0899	0.5234
0.68	1636	273.6	0.1023	0.5096
0.72	1568	264.2	0.1061	0.5024
0.76	1482(13)	251.4(2.1)	0.1161(10)	0.4944(23)
0.8	1407	239.5	0.1248	0.4877
0.84	1309(50)	227.8(3.4)	0.1366(26)	0.4789(19)
0.9	1043	188.0	0.1673	0.4716
0.96	863.8	157.1	0.2029	0.4602
1.0	693.9	130.0	0.2304	0.4553
1.1	473.4	85.9	0.3139	0.4394
1.2	317.2	66.6	0.3825	0.4165
1.4	205.9	55.8	0.4954	0.3329
1.6	188.3	60.3	0.5196	0.2991
2.0	161.4	52.3	0.5505	0.2884
		$\lvert\epsilon_g/\epsilon_a\rvert = 1$		
0.2	1972	316.6	0.0733	0.5985
0.3	1948	315.8	0.0798	0.5815
0.4	1743	283.0	0.0932	0.5667
0.45	1636	271.3	0.1011	0.5573
0.5	1527	255.6	0.1116	0.5485
0.55	1369	236.8	0.1253	0.5391
0.6	1183	205.4	0.1462	0.5362
0.7	811.9	149.9	0.2068	0.5238
0.75	591.4	115.0	0.2465	0.5149
0.8	462.7	95.5	0.2937	0.5093
0.9	270.7	64.1	0.3708	0.4910
1.0	209.4	53.1	0.4473	0.4419
1.5	89.3	41.1	0.5330	0.4107
2.0	47.4	40.8	0.5395	0.4061

[a] Standard error of simulation; 2148(11) means $2148 \pm (11)$.
[b] Stable random coil state obtained from cooling sequence.
[c] Stable collapsed structure obtained from heating sequence.
[d] Data for $\langle R^2\rangle$ in the ordered state has a large relative error, but the absolute error is only a few times larger than for the expanded state. In this case $\langle S^2\rangle$ is more reliable than $\langle R^2\rangle$.

distribution within the coil were also analyzed.

The average values of the most important conformational quantities ($\langle R^2\rangle$, $\langle S^2\rangle$, $\langle \nu\rangle$, and $\langle f_g\rangle$) for chain lengths $n = 50$, 100, 200, 400, and 800 are listed in Tables I–V. The most extensive computations were made for chain lengths $n = 200$ and $n = 400$ over a wide range of potential energy parameters of the model, while more limited parameter sampling was performed for the shorter chains and for

TABLE IV. Average properties of chains of length $n = 400$.

ϵ_g/k_BT	$\langle R^2\rangle$	$\langle S^2\rangle$	$\langle v\rangle$	$\langle f_g\rangle$
		$\lvert\epsilon_g/\epsilon_a\rvert = 4$		
0.0	4882(31)[a]	777.8(2.4)	0.0609(2)	0.6285(3)
0.5	5448	867.2	0.0496	0.5253
0.8	6033	964.1	0.0431	0.4599
1.0	6072(113)	985.6(22.1)	0.0390(5)	0.4158(5)
1.4	7639	1231.1	0.0316	0.3315
1.8	8790	1436.0	0.0286	0.2505
2.0($T\downarrow$)[b]	11010	1755.1	0.0395	0.2142
2.0($T\uparrow$)[c]	(1370)[d]	539.6	0.4991	0.1002
2.1	(658)	538.5	0.4274	0.1177
2.2	(1156)	561.0	0.4957	0.0988
2.4	(307.0)	466.6	0.5488	0.0865
		$\lvert\epsilon_g/\epsilon_a\rvert = 3$		
0.45	5155	832.1	0.0538	0.5385
0.6	5237	846.2	0.0524	0.5058
0.9	5497	904.6	0.0486	0.4418
1.2	5898	974.1	0.0469	0.3771
1.5	6547	1086.8	0.0496	0.3146
1.74($T\downarrow$)[b]	5988	999.1	0.0690	0.2694
1.74($T\uparrow$)[c]	(1530)	277.7	0.4721	0.1474
1.8	(1085)	232.7	0.4704	0.1580
1.95	(764)	175.8	0.4987	0.1503
2.1	(1429)	158.9	0.5351	0.1377
2.4	(1562)	154.0	0.5471	0.1373

[a–d] See footnotes to Table III.

the longest one, $n = 800$. This allows us to discuss the effect of chain length together with the effect of stiffness, quality of solvent and/or the temperature on chain conformation and the character of collapse transition. The independent variable in our simulations is the dimensionless ratio ϵ_g/k_BT, the reduced conformational energy of a *gauche* isomeric state. For a given ratio of ϵ_g to ϵ_a, the nearest neighbor interaction parameter, we computed $\langle R^2\rangle$, $\langle S^2\rangle$, $\langle v\rangle$, and $\langle f_g\rangle$ [Eqs. (10), (11), (7), and (8), respectively]. Together with the chain length n, the two last parameters determine the configurational energy of the model system. For a small subset of results, we give the numerical values of the standard deviation of the mean values listed in Tables I–V. Three independent MC runs were used for this purpose. In general the data for the expanded state above the collapse temperature are more accurate, with the relative statistical error of $\langle R^2\rangle$ and $\langle S^2\rangle$ below 2% in most cases. The error of $\langle v\rangle$ is generally below 1% and the error of $\langle f_g\rangle$ is well below 1% of the mean value. At low temperatures below the collapse transition, the uncertainty in the data is larger. The values of

TABLE V. Average properties of chains of length $n = 800$.

ϵ_g/k_BT	$\langle R^2\rangle$	$\langle S^2\rangle$	$\langle v\rangle$	$\langle f_g\rangle$
		$\lvert\epsilon_g/\epsilon_a\rvert = 4$		
0	11 223(52)	1757(7)	0.0675(23)	0.6279(4)
1.0	12 738(242)	2067(24)	0.0470(4)	0.4154(11)
1.4	15 265(613)	2443(90)	0.0453(46)	0.3304(4)
1.6	15 648(484)	2534(25)	0.0446(52)	0.2904(5)

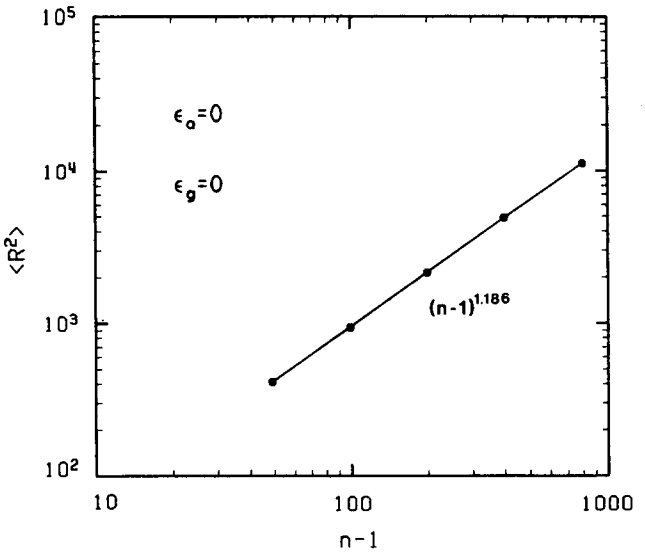

FIG. 1. Log–log plot of the mean-square end-to-end distance $\langle R^2\rangle$ vs chain length $n - 1$ for the SAW ($\epsilon_g = 0$ and $\epsilon_a = 0$).

$\langle R^2\rangle$ for the lowest flexibility system below the transition especially exhibit a significant scatter (these values have been listed in parentheses, and only the order of magnitude should be considered valid). However, even here, the *absolute* error of $\langle R^2\rangle$ is only few times larger than that observed in high temperature range.

The data in the first row of every Tables I–V correspond to the case of simple athermal SAW's on the diamond lattice ($\epsilon_g = \epsilon_a = 0$). It gives us an opportunity to compare our results with the results of previous work and provides a test of the sampling method used in present computations. In Fig. 1 the mean-square end-to-end separation $\langle R^2\rangle$ has been shown as a log–log plot vs the number of bonds $(n - 1)$. Our results for the case of an athermal system are well fit by $\langle R^2\rangle = A(n-1)^{\gamma}$ with $A = 4.037$ and $\gamma = 1.186$, which is in good agreement with other theoretical and numerical

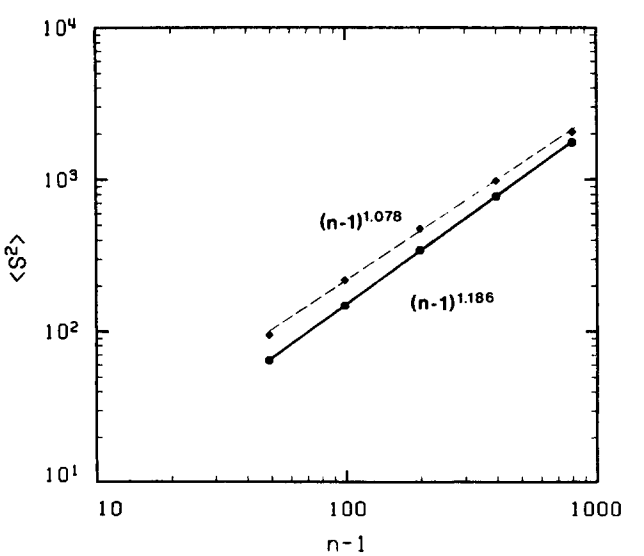

FIG. 2. Log–log plot of the mean-square radius of gyration, $\langle S^2\rangle$ vs chain length $(n - 1)$ for the SAW ($\epsilon_g = 0$ and $\epsilon_a = 0$) and for a stiff polymer ($\lvert\epsilon_g/\epsilon_a\rvert = 4$) at $\epsilon_g/k_BT = 1$.

work. For example, the above can be compared with $\gamma = 1.184 \pm 0.004$ of Ref. 30.

The main interest of the present studies is the effect of chain stiffness and of solvent quality on the properties of finite length chains. However a limited analysis of the effects of chain length can also be done using the data in Tables I–V. In Fig. 2, the chain length dependence of the mean-square radius of gyration $\langle S^2 \rangle$ is compared for a flexible athermal SAW ($\epsilon_g = \epsilon_a = 0$) in the solid curve with the corresponding dependence for relatively stiff polymers in a moderately poor solvent ($\epsilon_a = -\epsilon_g/4$) in the dashed curve. The data for the athermal SAW is well fit by a power law relation similar to that used for $\langle R^2 \rangle$ in Fig. 1 ($\gamma = 1.186$). The semiflexible polymers also seem to satisfy a power law with a smaller value of the exponent γ. The value $\gamma = 1.078$ for the case $\epsilon_g/k_B T = 1$, $|\epsilon_g/\epsilon_a| = 4$ is considerably smaller than is observed for a chain of unlimited flexibility with the same lattice restrictions, the same attractive force and a similar range of chain lengths.[13] This shows that limiting the flexibility for finite length chains leads to a significant decrease of the excluded volume effect on the coil dimensions. Note that an extrapolation to large n limit of this case with $\epsilon_a/k_B T = -0.25$ suggests that an attractive interaction of the magnitude $|\epsilon_g/\epsilon_a| = 4$ would compensate for the effect of local stiffness on the chain dimensions and results in an athermal SAW for chains of the order of $\sim 2 \times 10^3$ statistical segments. However, it is not clear if such an extrapolation is valid, i.e., that the exponent found in the window of $n = 100$ to $n = 800$ for semiflexible chains holds in the limit of infinitely large n.

We now wish to look at the temperature behavior of the excluded volume as a function of the flexibility of the polymer chain. We shall compare the MC results to an ideal RIS model.[31] The mean square radius of gyration for a finite length chain on a diamond lattice is given in the RIS model by

$$\langle S^2 \rangle / l^2 (n-1) = \frac{1}{6}\left(\frac{n+1}{n}\right)\left(\frac{1+\mu}{1-\mu}\right)\left(\frac{1+\eta}{1-\eta}\right) - \frac{\mu\eta + \lambda_1}{\lambda_1 - \lambda_2} Q_1 + \frac{\mu\eta + \lambda_2}{\lambda_1 - \lambda_2} Q_2 , \tag{12a}$$

with

$$Q_1 = \frac{\lambda_1}{n(1-\lambda_1)^2}\left[1 - \frac{2\lambda_1}{n(1-\lambda_1)} + \frac{2\lambda_1^2(1-\lambda_1^{n-1})}{n(n-1)(1-\lambda_1)^2}\right] \tag{12b}$$

and

$$Q_2 = \frac{\lambda_2}{n(1-\lambda_2)^2}\left[1 - \frac{2\lambda_2}{n(1-\lambda_2)} + \frac{2\lambda_2^2(1-\lambda_2^{n-1})}{n(n-1)(1-\lambda_2)^2}\right] . \tag{12c}$$

Here, $\mu = \cos(\theta)$ the bond angle parameter (in the case of a diamond lattice $\mu = 1/3$; $\eta = \langle \cos\phi \rangle$, the average rotational angle, which for a chain on a diamond lattice can be computed from

$$\eta = \frac{1 - \exp(-\epsilon_g/k_B T)}{1 + 2\exp(-\epsilon_g/k_B T)} \tag{12d}$$

and λ_1 and λ_2 are the two first eigenvalues of the Flory averaged rotation matrix

$$\lambda_{1,2} = \tfrac{1}{2}\{\mu(1-\eta) \pm [\mu^2(1-\eta)^2 + 4\eta]^{1/2}\} . \tag{12e}$$

In Fig. 3 we compare the temperature dependence of $\langle S^2 \rangle$ for the ideal RIS model [as given by Eq. (12)] with a

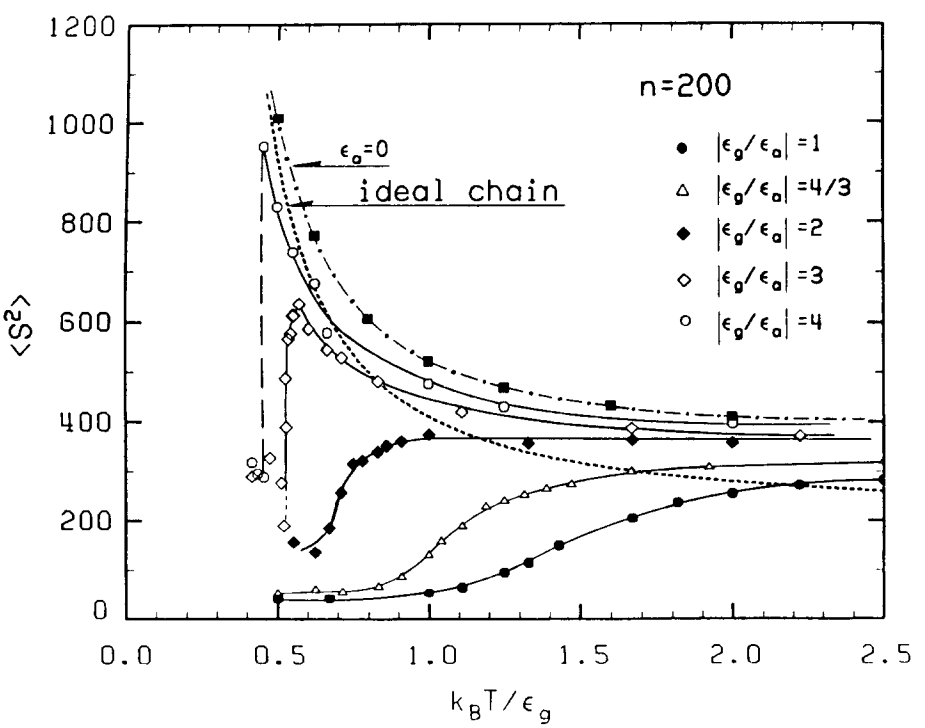

FIG. 3. The temperature dependence of the mean-square radius of gyration for a chain composed of $n = 200$ beads with various ratios of the stiffness parameter ϵ_g to the attractive interaction ϵ_a. The dotted line corresponds to the theoretical results for the RIS model [Eq. (12)]. The points where the lines obtained from a smooth interpolation of the MC data intercept the theoretical one for an ideal RIS chain gives the θ temperature for the system under consideration.

semiflexible polymer in an athermal solvent ($\epsilon_a = 0$ but with excluded volume), and with three examples of a semiflexible polymer with an attractive force (poor solvent case) for $n = 200$. It can be noted that with decreasing temperature (which decreases the flexibility of the chain backbone) the ideal and excluded volume athermal polymer results approach each other. This means that the excluded volume effect on polymer size for fixed chain length decreases with increasing stiffness. In treating polymers with nonzero attractive interactions, the degree of stiffness of the polymer is given by the relative strengths of the attractive interaction and the *gauche–trans* energy separation—that is by the ratio $|\epsilon_g/\epsilon_a|$. When $|\epsilon_g/\epsilon_a|$ is large, the polymer is quite stiff and expands with decreasing temperature, very much as was the case without attractive interactions, until at some critical temperature the stiff polymer chain suddenly collapses. This is illustrated in Fig. 3 for $|\epsilon_g/\epsilon_a| = 4$. Flexible polymers, on the other hand, show a monotonic decrease in size with decreasing temperature and the collapse to a tight random coil is continuous. This is illustrated in Fig. 3 for $|\epsilon_g/\epsilon_a| = 1$. The borderline case (between stiff and flexible) where the chain size is essentially temperature independent over a wide temperature range until the collapse (which now occurs continuously over a relatively narrow temperature range) is illustrated in Fig. 3 for $|\epsilon_g/\epsilon_a| = 2$. This general behavior can be quite readily understood. At very high temperature ($k_B T/\epsilon_g \to \infty$) the energetic parameters are unimportant and all chains obey self-avoiding random walk statistics. For a stiff polymer, as we decrease the temperature the energetic bias of *trans* states over *gauche* begins to take over and rotational degrees of freedom are frozen out. As *trans* stretches begin to appear, the polymer slowly unfolds itself from the completely flexible random coil configuration and the size increases. As the temperature further decreases the stiff polymer collapses into an ordered configuration since it can decrease its free energy by having a large number of attractive interactions at the expense of only a small number of *gauche* states (bends). This will be further illustrated below in Sec. III C where we discuss the nature of the collapsed state. Any polymer with nonzero attractive interactions seems to eventually collapse if it is long enough (if it is not, it becomes a stiff rod). For flexible polymers, as the temperature is lowered the attractive forces dominate, and the polymer decreases its free energy by contracting, increasing the energetic contribution to the free energy at the expense of the entropic term. Thus, the difference in the temperature behavior depends on whether local rotational degrees of freedom (stiff polymer chain) or the effective size of configurational space (flexible polymer chain) closes down first.

The critical collapse temperature T_c is well defined for stiff polymers. The estimated values of $k_B T_c/\epsilon_g$ are compared in Table VI for the most extensively studied systems of $n = 200$ and $n = 400$ for $|\epsilon_g/\epsilon_a| = 3$ and 4. Since the collapse from an expanded random coil to a compact random coil is continuous for the more flexible polymers we do not estimate T_c for these systems. Table VI also contains approximate values (the statistical error is unity in the last digit) of the theta point ($k_B\theta/\epsilon_g$) estimated as the point where repulsive interactions are compensated by attractive

TABLE VI. Critical values of $k_B T_C/\epsilon_g$ and the θ point estimated from $\langle S^2\rangle$ dependence on $k_B T/\epsilon_g$.

Chain length	$\lvert\epsilon_g/\epsilon_a\rvert$	$k_B T_C/\epsilon_g$	$k_B\theta/\epsilon_g$	$k_B\theta/\epsilon_a$
$n = 200$	4	0.45	0.63	2.50
200	3	0.53	0.83	2.50
200	2	...	1.19	2.38
200	4/3	...	1.72	2.30
200	1	...	2.22	2.22
$n = 400$	4	0.50	0.62	2.46
400	3	0.57	0.83	2.50
$n = 800$	4	...	0.66	2.65

ones, and the simulated mean square radius of gyration, $\langle S^2\rangle$ becomes the same as the RIS model $\langle S^2\rangle$ given by Eq. (12). For ease of comparison with previous MC work on flexible polymers we also list the corresponding values of $k_B\theta/\epsilon_a$. It can be noted that the θ point as a function of ϵ_a increases as the chain stiffness increases. In other words, a smaller attractive force per segment is necessary to compensate for the hard core repulsions in stiff polymers, than in more flexible ones. Actually all the values of $k_B\theta/\epsilon_a$ (with the exception of the most flexible polymer studied; $\epsilon_a = \epsilon_g$) are considerably greater than those found for the case of diamond lattice polymers of unlimited flexibility (i.e., $\epsilon_g = 0$ in our notation) which was estimated by Kremer *et al.*[12] to be 2.25 ± 0.05. Since the statistical accuracy of the present estimation of the θ point is also about ± 0.05 the observed shift of the θ temperature is significant and gives further evidence for the smaller importance of excluded volume in semiflexible polymers.

The qualitative difference between the behavior of flexible polymers and stiff ones can easily be observed in Fig. 3. The temperature dependence of polymer coil size of the range of high temperatures is different for the two kinds of systems. Moreover the sharp, discontinuous, collapse with a distinct region of metastable states is present for stiff chains. This is in qualitative agreement with the analytical results of Post and Zimm.[21] Sanchez's[3] mean field theory prediction that the polymer collapse transition is second order does not contradict our findings since he assumes *a priori* a highly flexible chain. Our MC results also show a smooth gradual collapse transition for flexible polymers.

The behavior of the expansion parameter with chain length can best be illustrated by comparing the data for $|\epsilon_g/\epsilon_a| = 3.0$ in Figs. 3 and 4 for $n = 200$ and $n = 400$. For $n = 200$ the $\langle S^2\rangle$ dependence on temperature for $|\epsilon_g/\epsilon_a| = 3.0$ clearly is behaving like a stiff polymer, while for $n = 400$ it has almost become a borderline case. The reason for this change in character with increasing chain length will be discussed in the next subsection when we discuss the nature of the collapsed state.

It might at first appear to be somewhat disturbing that in some of the systems we simulated the mean-square radius of gyration has a value larger after the collapse transition than that for an ideal chain of unlimited flexibility, namely $\langle S^2\rangle_0 = 198$ and 398 for chains of $n = 200$ and 400, respec-

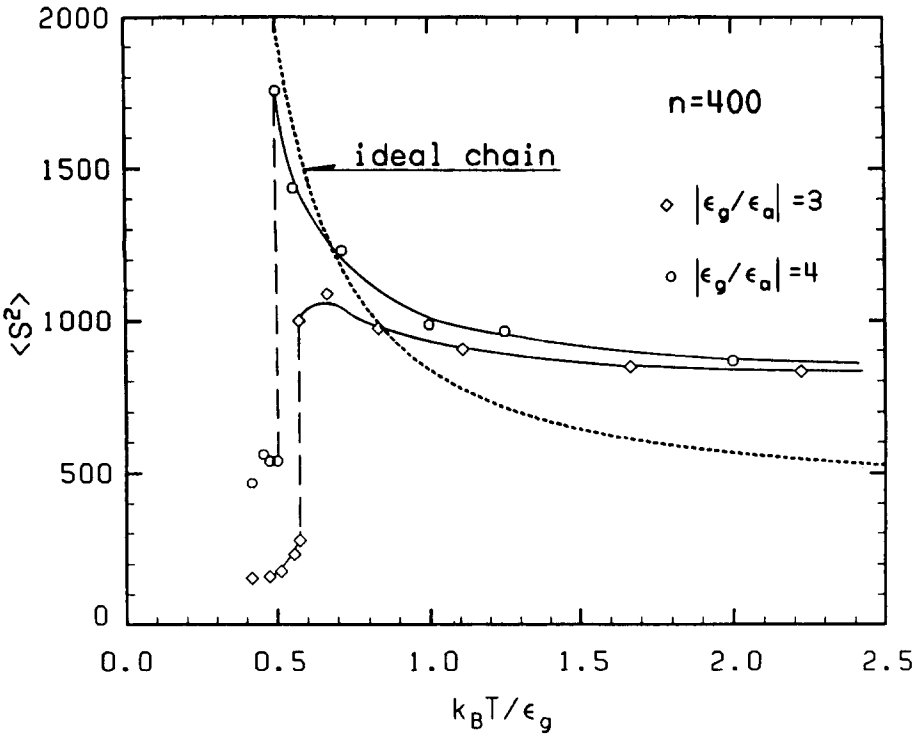

FIG. 4. The temperature dependence of the mean-square radius of gyration for a chain composed of $n = 400$ beads with various ratios of the stiffness parameter ϵ_g to the attractive interaction ϵ_a. The dotted line corresponds to the theoretical results for the RIS model [Eq. (12)]. The points where the lines obtained from a smooth interpolation of the MC data intercept the theoretical one for an ideal RIS chain gives the θ temperature for the system under consideration.

tively. This has been observed for $n = 200$ system for $|\epsilon_g/\epsilon_a| = 3.0$ and 4.0 and for $n = 400$ for $|\epsilon_g/\epsilon_a| = 4.0$. This is caused by the particular ordered structure of the collapsed state which is discussed later.

B. Comparison with mean-field theory

As mentioned above, mean-field lattice theory has been shown to be able to reproduce the qualitative difference between the collapse of flexible and stiff polymers if one includes third order terms in the virial expansion. Following Post and Zimm[21] the expansion factor α_R at the free energy minimum can be obtained as

$$\alpha_R^8 - \alpha_R^6 - Cz\alpha_R^3 = y\,, \tag{13a}$$

with $\sigma_R^2 = \langle R^2_{\rm MC}\rangle/\langle R^2_{\rm RIS}\rangle$, where the subscript MC indicates the MC results and RIS the dimension of the rotational isomeric state model with no excluded volume but with the proper stiffness for the temperature of interest. C is the Flory constant, equal to $3^{3/2}$ and z and y are related to the virial coefficients B_2 and B_3 by

$$z = 2^{-1/2}(3/\pi)^{3/2}B_2 n^{1/2}\omega^3 \tag{13b}$$

and

$$y = 3^{3/2}(3/\pi)^3 B_3\omega^6\,. \tag{13c}$$

Here ω is related to the actual length of the statistical segment via

$$\omega^6 = V_P^3/\langle R^2_{\rm RIS}\rangle^3/V_1 \tag{13d}$$

and reduces to $(n/\langle R^2_{\rm RIS}\rangle)^3$ for the lattice model, where $V_P = n$ is the polymer molecular volume and $V_1 = 1$ is the solvent molecular volume.

The virial coefficients B_2 and B_3 can be expressed in the terms of the binary cluster integrals

$$B_2 = (1 - q\xi)/2 \tag{14a}$$

and

$$B_3 = (1 + 3q\xi^2 - 2q\xi^3)/3\,, \tag{14b}$$

with $q = 4$ the coordination number of the diamond lattice, and

$$\xi = \left\langle \exp\left(-\frac{w_{ij}}{k_B T}\right) - 1 \right\rangle. \tag{14c}$$

We assume that the potential of mean force w_{ij} between segments i and j has the form of a free energy

$$-\frac{w_{ij}}{k_B T} = (f - Ts)\epsilon_g/k_B T\,. \tag{15}$$

Treating f and s as adjustable parameters we fit our MC data for α_R^2 to Eq. (13). The fit seems to be excellent for stiff polymers giving the correct reproduction of the discontinuous collapse and quite satisfactory for more flexible chains. A sample comparison of the theoretical α_R^2 and MC results is given in Table VII. The values of adjustable parameters f and s are given in Table VIII together with the statistical error of the fit. Inspection of the data from Table VII shows that both the energetic and entropic (the term associated with Ts) contribution to the potential of mean force decrease with increasing chain stiffness. At high temperatures the entropic term dominates, while at low temperatures the energetic term dominates. Comparison of the $n = 200$ with $n = 400$ results indicates that both f and s are essentially molecular weight independent. In the vicinity of the θ temperature, the resulting value of the second virial coefficient [Eq. 14(b)] is close to zero while B_3 is positive, in agreement with conventional wisdom.[18,19,21]

Hence, it can be concluded that the mean field theory of Post and Zimm[21] describes our computational experiments very well as far as the global characteristics of polymer dimensions are concerned. This is somewhat surprising since

TABLE VII. Comparison of the MC data with mean-field Post–Zimm (Ref. 21) semiempirical predictions of the expansion factor, $n = 200$.

$\lvert\epsilon_g/\epsilon_a\rvert = 4$			$\lvert\epsilon_g/\epsilon_a\rvert = 1$		
ϵ_g/k_BT	α_R^2 (MC)[a]	α_R^2 (theory)[b]	ϵ_g/k_BT	α_R^2 (MC)[a]	α_R^2 (theory)[b]
0.5	1.4687	1.4700	0.2	1.4470	1.4471
0.8	1.3348	1.3351	0.3	1.3314	1.3319
1.0	1.1711	1.1711	0.4	1.1075	1.1145
1.5	0.9342	0.9499	0.45	1.0016	1.382
1.6	1.0101	0.9977	0.5	0.9003	0.8458
1.8	0.9271	0.9227	0.525	0.8719	0.8391
2.0	0.8777	0.8745	0.55	0.7771	0.7501
2.2($T\downarrow$)	0.8441	0.8415	0.6	0.6462	0.6232
2.2($T\uparrow$)	0.0909	0.0827	0.7	0.4102	0.3858
2.3	0.1415	0.1356	0.75	0.2872	0.2587
			0.8	0.2159	0.1831
			0.9	0.1165	0.0690
			1.0	0.0830	0.0177

[a] α_R defined in text below Eq. (13).
[b] See text Sec. III B.

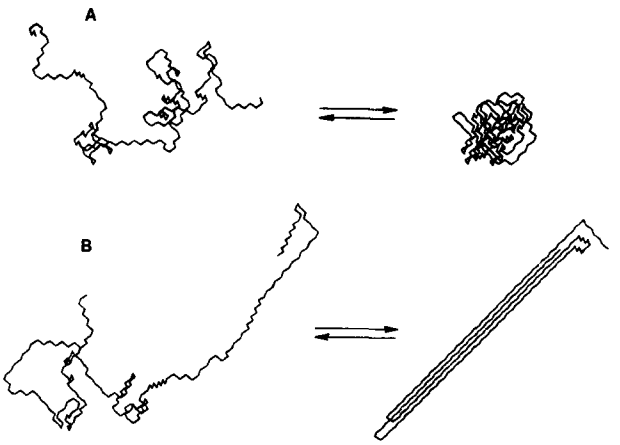

FIG. 5. (A). Collapse of a flexible polymer, $\lvert\epsilon_g/\epsilon_a\rvert = 1$. (B). Collapse of a stiff polymer, $\lvert\epsilon_g/\epsilon_a\rvert = 4$.

the mean field theory treats the dense collapsed states as a random coil while, as we shall show in the next section, stiff polymers collapse to a well defined ordered structure rather than to a high density, essentially Gaussian coil.

C. The effect of stiffness on the structure of the collapsed state

Most of the theories of the polymer collapse from an expanded coil to a globular state of higher density assume that the character of the polymer segment distribution is qualitatively the same in both phases. The density of the polymer is the only parameter which distinguishes the two states. This behavior was observed in the present studies for polymer models which had substantial flexibility of the chain backbone. However the character of the collapsed state for less flexible polymers is qualitatively different. The low temperature state is not a random coil of high density. This is schematically shown in Fig. 5 where representative snapshot projections of the polymer conformation before and after the collapse transition are shown for the two systems of high (A) and low (B) flexibility of the chain. The difference is evident. It should be noted that Fig. 5(A) shows the polymer conformation separated by a temperature increment (because the transition is a smooth one) while both the conformations in Fig. 5(B) correspond to exactly the same reduced temperature k_BT/ϵ_g.

As was mentioned above, the low temperature structure of stiff model polymers is highly ordered with a relatively well defined shape of a bundle of folded long *trans* stretches. The ratio $\lvert\epsilon_g/\epsilon_a\rvert$ seems to determine the length of the rodlike bundle. In several "cooling–heating" computational experiments, we always observed that the structure was composed of 4–6 stretches for the chain length $n = 200$ and 9–12 stretches for $n = 400$ when $\lvert\epsilon_g/\epsilon_a\rvert = 4.0$. The slightly more flexible polymer with $\lvert\epsilon_g/\epsilon_a\rvert = 3.0$ also collapsed to a relatively well defined structure characterized by a somewhat larger average number of folds. In contrast, the low temperature conformation of more flexible chains resembles a random coil with a high density of polymer segments. This effect is demonstrated in Table IX where the average length of the *trans* sequences has been listed for a flexible chain of length $n = 200$ and stiff chain of length $n = 200$ and $n = 400$ at the same set of temperatures. The first important conclusion which can be drawn from inspection of the numerical data of Table IX is that the abrupt collapse of semiflexible polymers induces considerably more stiffness. However, as shown below the collapse of flexible polymers leaves the observed flexibility (fraction of *gauche* states and the distribution of such sequences) frozen at a level characteristic of a higher temperature. These two qualitatively distinct behaviors have been compared with the average number of *gauche* states for an ideal RIS model as a function of temperature in Fig. 6 for chains with $n = 200$. Here we see that for stiff chains (e.g., $\lvert\epsilon_g/\epsilon_a\rvert = 4$) at high temperatures the fraction of *gauche* states while starting out slightly below the ideal RIS results behaves qualitatively like the RIS model until the collapse temperature where it discontinuously drops. On the other hand, for flexible chains (e.g., $\lvert\epsilon_g/\epsilon_a\rvert = 1$), as the temperature decreases f_g does not behave qualitatively like the ideal RIS model but rather tends to flatten out, becoming relatively temperature insensitive.

TABLE VIII. Values of the adjustable parameters f and s [Eq. (15)] and estimated error of the fit.

Chain length	$\lvert\epsilon_g/\epsilon_a\rvert$	f	$s\epsilon_g/k_B$	$\sigma^2\times10^3$ [a]
$n = 200$	4	0.4138	0.1035	2.26
200	3	0.4397	0.0953	0.16
200	2	0.5305	0.1220	0.57
200	4/3	0.8033	0.1994	3.58
200	1	0.973	0.2269	1.80
$n = 400$	4	0.4503	0.1082	2.43
	3	0.5253	0.1238	0.86

[a] Mean square residual for the quantity $\alpha_{MC}^8 - \alpha_{MC}^6 - (cz\alpha_{MC}^3 + y)$.

TABLE IX. Mean length of *trans* sequences.

	$n=200, \lvert\epsilon_g/\epsilon_a\rvert=1$		$n=200, \lvert\epsilon_g/\epsilon_a\rvert=4$		$n=400, \lvert\epsilon_g/\epsilon_a\rvert=4$	
ϵ_g/k_BT	n_t[a]	$\langle n_t\rangle$[b]	n_t	$\langle n_t\rangle$	n_t	$\langle n_t\rangle$
0	1.528	2.069	1.528	2.069	1.529	2.073
0.5	1.815	2.633	1.852	2.723	1.853	2.725
0.8	1.985	2.867	2.117	3.243	2.131	3.284
1	2.445	3.751	2.360	3.746	2.376	3.767
1.5	2.705	3.856	3.200	5.4078	...	...
2	2.681	3.920	4.661	8.297	4.716	8.520
(2)[c]	...	...	...	...	(14.16)	(34.63)
2.2	...	...	5.593	10.39	...	...
(2.2)[c]	...	...	(22.48)	(35.09)	(15.80)	(35.19)

[a] Arithmetic average of the number of bonds in a *trans* sequence.
[b] Weighted average $\langle n_t\rangle = (1/f_t)\cdot\Sigma_{i=1}^{n-3} i f_{t,i}$, where $f_{t,i}$ is the average fraction of *trans* states in a sequence of length i.
[c] The numbers in parentheses are for the ordered, collapsed phase.

In Fig. 7 an example of the change of distribution of the sequence of conformational states at the collapse transition has been shown for a stiff chain with $n=200$, $|\epsilon_g/\epsilon_a|=4.0$, by plotting $f_{t,i}$, the average fraction of *trans* states in a sequence of length i vs i. The *trans* sequence distribution for the expanded coil state is close to that predicted by the RIS model. The spectrum for the collapsed structure (at the same temperature) exhibits a discrete distribution of lengths of *trans* stretches with the larger peak corresponding to the long stretches down the bundle and the smaller peak due to the contribution of the folds.

In Fig. 8, we show another comparison of an "order parameter" of the chain conformation of polymers with $n=200$ of varying degrees of flexibility. Here, we plot the average number of nonbonded nearest neighbor pairs per polymer segment $\langle\nu\rangle$ as a function of temperature. For the stiffer polymer chains, $\langle\nu\rangle$ jumps discontinuously from a value close to zero above the transition to a large value at the collapse transition. On the other hand for the more flexible chains the number of nonbonded pairs gradually rises monotonically as the chain dimensions decrease.

Our general picture quite readily explains this behavior. For the stiffer chains, as discussed in Sec. III A, the rotational degrees of freedom freeeze out as the temperature de-

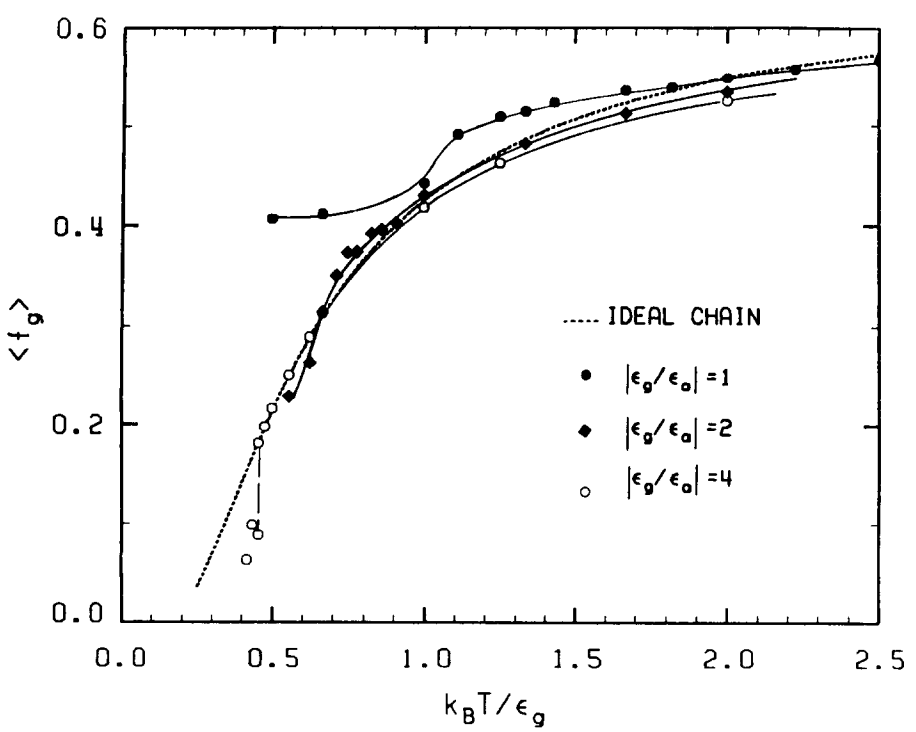

FIG. 6. The temperature dependence of the fraction of *gauche* states in chains of $n=200$ for various ratios of the stiffness parameter ϵ_g to the attractive interaction ϵ_a. The dotted line corresponds to the theoretical results for the RIS model.

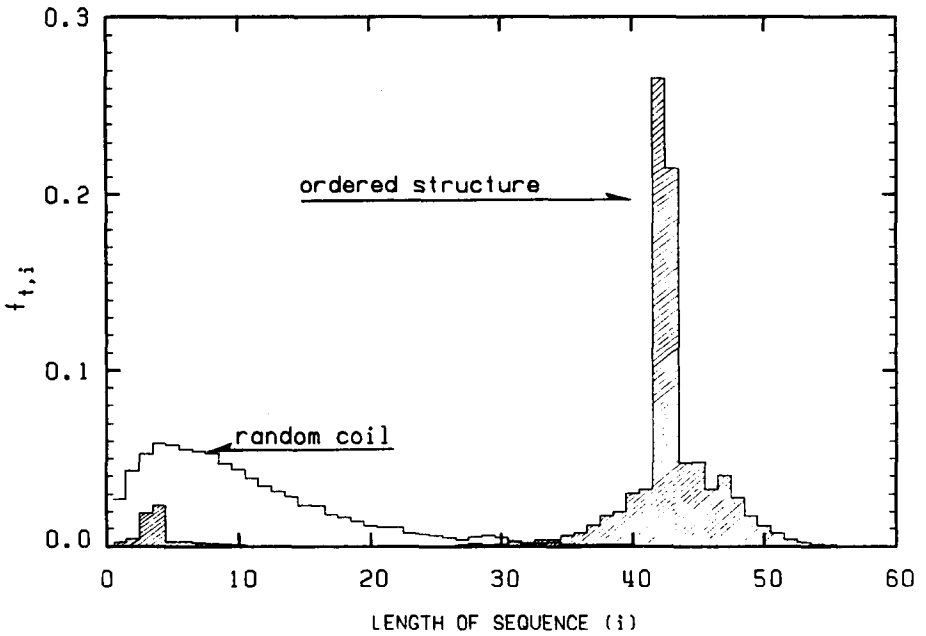

FIG. 7. The comparison of the *trans* sequence distribution at the collapse transition for a stiff chain ($|\epsilon_g/\epsilon_a| = 4$), $n = 200$. Both superimposed diagrams correspond to exactly the same temperature $k_B T/\epsilon_g = 0.455$.

creases, thus leading to a series of all *trans* stretches. For example, a chain of $n = 200$ with a stiffness parameter $|\epsilon_g/\epsilon_a| = 4$ has approximately 15–20 *trans* stretches just above the collapse transition. Hence, the chain just above the transition behaves as if it were a "small molecule" composed of (about) 15 stiff sections connected by "flexible" linkages. It is therefore a simple matter for this small molecule to sample configuration space to find a free energy minimum by increasing the contacts and decreasing the size of the bends in the ordered structure. In a sense the polymer chain is preformed for readily finding the ordered collapsed structure. It should be noted that the length of *trans* stretches is a function of the stiffness parameter $|\epsilon_g/\epsilon_a|$, not of the chain length. Thus, as the chain length increases, the polymer chain above the collapse transition has an increasing number of *trans* stretches and behaves less and less like a small molecule. This is why the chain with the stiffness parameter $|\epsilon_g/\epsilon_a| = 3.0$ behaves as a stiff chain at chain length $n = 200$ but is closer to a borderline case where $n = 400$. A consequence of this is that in the $n \to \infty$ limit, for any finite value of

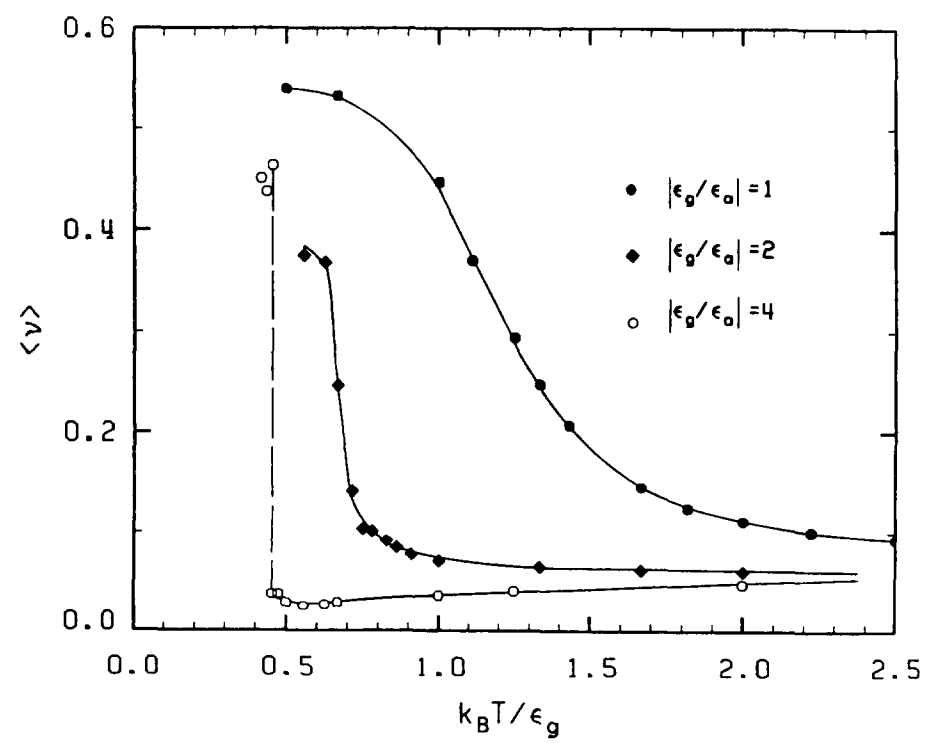

FIG. 8. The temperature dependence of the average number of nearest neighbor pairs per polymer segment [Eq. (7)] for polymers of various flexibility, $n = 200$.

$|\epsilon_g/\epsilon_a|$, the chain will collapse into a globally disordered state. Thus, the apparent first order transition seen for stiff systems at fixed finite $|\epsilon_g/\epsilon_a|$ is most likely a finite length effect, and not a true thermodynamic first order phase transition. If the chain is stiff there will be locally parallel *trans* stretches as in Fig. 5(B), but globally it will look like Fig. 5(A) with a change of distance scale.

The flexible chains continuously decrease their sizes as the temperature decreases and thus continuously increase the average number of nonbonded neighbor contacts. This increase of the number of contacts tends to freeze the *gauche* to *trans* ratio at a value that is characteristic of an ideal RIS chain at a higher temperature.

A self-consistent treatment of the collapse transition for stiff chains can be obtained by utilizing the fact that just above the transition the number of nearest neighbor contacts is small (see Fig. 8) and the chain is well described by the RIS model. Hence above the transition the free energy A_d is dominated by the entropic contribution which can approximately be evaluated using the RIS model. Below the phase transition, there are only a small number of loops [see Fig. 5(B)] and the free energy for the ordered collapsed structure A_0 can be well approximated by the internal energy using the observed number of contacts and by neglecting the entropic contribution. Using these approximations

$$A_d = -k_B T(n-3)\ln[1+2\exp(-\epsilon_g/k_B T)] + n\nu_d\epsilon_a \tag{16}$$

for the expanded state and

$$A_0 = n\nu_0\epsilon_a \tag{17}$$

for the collapsed state. In Eq. (16) [17] ν_d [ν_0] refers to the disordered [ordered] state and is obtained from the simulation. Equating Eqs. (16) and (17) allows us to calculate the transition temperature T_c. In Table X we present results for $n = 200$ and $n = 400$. This simple approach works very well for the $|\epsilon_g/\epsilon_a| = 4.0$ case where the intrinsic stiffness of the chains is particularly dominant, and not so well for the $|\epsilon_g/\epsilon_a| = 3.0$ case, where the local chain stiffness is not pronounced prior to the collapse.

These calculations thus lend further support to the contention that the collapse transition at finite n is apparently discontinuous for chains of sufficient conformational stiffness. Other measured quantities such as higher moments of the end-to-end distance distribution, higher moments of the radius of gyration distribution, the heat capacity obtained from the fluctuations in the configurational energy of the system, and the segment–segment order parameter (as measured by the second Legendre polynomial) also exhibit the same qualitative differences for the collapse transition as a function of the stiffness parameter. In the interest of economy of presentation we have refrained from including a detailed presentation of these results since they are less important both for comparison with other theories and with experiment.

TABLE X. Comparison of calculated and observed collapse transition temperature.

$n =$	$\lvert\epsilon_g/\epsilon_a\rvert$	$k_B T_c/\epsilon_g$ [a] from theory	$k_B T_c/\epsilon_g$ from simulation
200	4	0.482	0.455
400	4	0.494	0.500
200	3	0.383	0.529
400	3	0.523	0.575

[a] Calculated by equating Eqs. (16) and (17).

V. SUMMARY

Using Monte Carlo methods we have numerically studied the conformation of a single polymer chain with excluded volume on a diamond lattice for finite chains with lengths ranging from 50 to 800 monomer units over a wide range of local conformational stiffness. This was done in order to find out the effects of varying the stiffness on finite length polymers with both repulsive (excluded volume) and attractive interactions. The major new result of this work is that broadly speaking polymers separate into two classes loosely referred to here as flexible and stiff, each of which exhibits quite different qualitative behavior.

The more flexible polymer chains undergo a transition from a high temperature, extended random coil phase to a low temperature, high density, collapsed random coil phase. This is caused by the attractive interactions between nonbonded units. As the temperature decreases, the average number of nonbonded contacts between monomer units gradually increases resulting in a denser and less extended coil. At the same time, this increased density inhibits the formation of *trans* states and results in a *gauche* to *trans* ratio appreciably greater than ideal chain statistics would predict, (i.e., one which is frozen at a value characteristic of an ideal chain at a higher temperature).

The dimensions of the stiffer chains increase as the temperature decreases. This occurs because the freezing out of the rotational degrees of freedom dominates over the attractive interactions. Thus, the chain develops a sequence of stiff, all *trans*, stretches while it is still in its expanded random coil state. As the temperature is further decreased, the chain suddenly undergoes a pseudo-first-order phase transition and collapses to an ordered dense phase composed of a series of close packed, *trans* stretches with a minimum number of small bends. This tendency of stiff chains to collapse into an ordered dense state containing a high fraction of *trans* stretches is perhaps not dissimilar to certain aspects of the conformational transition in globular proteins and is further pursued elsewhere.[32]

ACKNOWLEDGMENTS

This research was supported in part by grants from the Biophysics Program, No. PCM-82-12404, and the Polymer Program, No. DMR-83-03197, of the National Science Foundation. Acknowledgment was made to the Monsanto Company for an institutional research grant for the purchase of a μVAXII computer on which the simulations reported

here were predominantly carried out.

[1]P. J. Flory, J. Chem. Phys. **17**, 303 (1949).
[2]S. F. Edwards, Proc. Phys. Soc. **85**, 613 (1965).
[3](a) I. M. Lifshitz, A. Y. Grosberg, and A. R. Khokhlov, Rev. Mod. Phys. **50**, 683 (1978); (b) I. C. Sanchez, Macromolecules **12**, 980 (1979).
[4]P. J. Flory and S. Fisk, J. Chem. Phys. **44**, 2243 (1966).
[5]See also review of S. G. Whittington, *Advances in Chemical Physics* (Wiley, New York, 1982), Vol. 51, Chap. 1 and references therein.
[6](a) P. G. de Gennes, *Scaling Concepts in Polymer Physics* (Cornell University, Ithaca, NY, 1979); (b) see also for example M. Muthukumar, J. Chem. Phys. **81**, 6272 (1984).
[7]M. E. Fisher and B. J. Hiley, J. Chem. Phys. **34**, 1253 (1961).
[8]D. C. Rapaport, Phys. Lett. A **38**, 339 (1974).
[9]D. C. Rapaport, J. Phys. A **10**, 637 (1977).
[10](a) J. Mazur and F. L. McCrackin, J. Chem. Phys. **49**, 648 (1968); (b) F. L. McCrackin, J. Mazur, and C. Guttman, Macromolecules **6**, 859 (1973).
[11]M. Jenssens and A. Bellemans, Macromolecules **9**, 303 (1976).
[12]K. Kremer, A. Baumgartner, and K. Binder, J. Phys. A **15**, 2879 (1981).
[13]A. Kolinski and A. Sikorski, J. Polym. Sci. Polym. Chem. Ed. **20**, 3147 (1982).
[14]See also review of A. Baumgartner in *Application of the Monte Carlo Method in Statistical Physics* (Springer, Berlin, 1984), Chap. 5.
[15]J. F. Douglas and K. F. Freed, Macromolecules **18**, 2445 (1985).
[16]C. Domb, Polymer **15**, 259 (1974).
[17]M. A. Moore, J. Phys. A **10**, 305 (1977).
[18]P. G. de Gennes, J. Phys. (Paris) **36**, L55 (1975).
[19]Y. Oono, J. Phys. Soc. Jpn. **41**, 228 (1976).
[20]M. Fixman and J. Skolnick, Macromolecules **11**, 863 (1978).
[21]C. B. Post and B. H. Zimm, Biopolymers **18**, 1487 (1979).
[22]H. Yamakawa and J. Shimada, J. Chem. Phys. **83**, 2607 (1985).
[23]T. M. Birshtein, A. M. Skvorcov, and A. A. Sariban, Macromolecules **10**, 202 (1977).
[24]H. Murakami, T. Norisuye, and H. Fujita, Macromolecules **13**, 345 (1980).
[25]M. F. Thorpe and W. K. Schroll, J. Chem. Phys. **75**, 5143 (1981).
[26]W. K. Schroll, A. B. Walker, and M. F. Thorpe, J. Chem. Phys. **76**, 6384 (1982).
[27]M. Gordon, P. Kapadia, and A. Malakin J. Phys. A **9**, 751 (1976).
[28]M. N. Rosenbluth and A. W. Rosenbluth, J. Chem. Phys. **23**, 356 (1955).
[29]H. Meirovitch, J. Phys. A **15**, L735 (1982).
[30]D. C. Rapaport, J. Phys. A **18**, 113 (1985).
[31]P. J. Flory, *Statistical Mechanics of Chain Molecules* (Wiley, New York, 1969).
[32]A. Kolinski, J. Skolnick, and R. Yaris, Proc. Natl. Acad. Sci. U.S.A. (to be published).